Integrating Tensile Parameters in Hexahedral Mass-Spring System for Simulation

V. Baudet, M. Beuve, F. Jaillet, B. Shariat, F. Zara

Université de Lyon, CNRS
Université Lyon 1,
LIRIS, SAARA team, UMR5205,
F-69622, Villeurbanne, France

firstname.name@liris.cnrs.fr

ABSTRACT

Besides finite element method, mass-spring systems are widely used in Computer Graphics. It is indubitably the simplest and most intuitive deformable model. This discrete model allows to perform interactive deformations with ease and to handle complex interactions. Thus, it is perfectly adapted to generate visually plausible animations. However, a drawback of this simple formulation is the relative difficulty to control efficiently physically realistic behaviors. Indeed, none of the existing models has succeeded in dealing with this satisfyingly. We demonstrate that this restriction cannot be over-passed with the classical mass-spring model, and we propose a new general 3D formulation that reconstructs the geometrical model as an assembly of elementary hexahedral "bricks". Each brick (or element) is then transformed into a mass-spring system. Edges are replaced by springs that connect masses representing the vertices. The key point of our approach is the determination of the stiffness springs to reproduce the correct mechanical properties (Young's modulus and Poisson's ratio) of the reconstructed object. We validate our methodology by performing some numerical experiments. Finally, we evaluate the accuracy of our approach, by comparing our results with the deformation obtained by finite element method.

Keywords

Discrete Modeling, Physical Simulation, Mass-Spring System, Rheological Parameters.

1 INTRODUCTION

Finite elements methods (FEM) are generally used to accurately simulate the behavior of 3D deformable objects. They require a rigorous description of the boundary conditions. The amplitudes of the applied strains and stresses must be well defined in advance to choose either a small - with Cauchy's description - or a large deformation context - with St Venant Kirchoff's description. Indeed, the accuracy of each context is optimized within its domain of deformation.

Mass-spring systems (MSS) have largely been used in animation, because of their simple implementation and their possible applications for a large panel of deformations. They consist in describing a surface or a volume with a mesh in which the global mass is uniformly distributed over the mesh nodes. The tensile behavior of the object is simulated by the action of springs, connecting the mesh nodes. Then, Newton's laws govern the dynamics of the model, and the system can be solved by solving Ordinary Differential Equations (ODEs) via numerical integration over time. In computer graphics, MSS based animations are generally proposed to deal with interactive applications and to allow unpredictable interactions. They are adapted to virtual reality environments where many unpredicted collisions may occur and objects can undergo deformations and/or mesh topology changes. Medical or surgery simulators present another example of their possible applications. Nevertheless these models generally fail to represent accurately the behavior of real objects, characterized by Young's modulus and Poisson's ratio (parameterization problem).

In this paper, our aim is not a comparative study of MSS and FEM models. The goal is to propose a new solution to enhance the MSS, making them more compatible with the requirements of physical realism. Section 2 presents a state of the art of mass-spring systems and particularly their parameterization. Moreover, in

this section, we present published solutions allowing the determination of springs constant to obtain a realistic behavior of the simulated object. Section 3 presents our approach to calculate stiffness constants of springs according to tensile parameters of the simulated object. Section 4 presents some experimental results. Finally, some concluding remarks and perspectives are given in section 5. Then, Appendix A provides a more detailed explanation of some results presented in section 3.2.

2 RELATED WORK

Mass-spring systems have been used to model textiles [KEH04, LJF+91, Pro95], long animals such as snakes, or soft organic tissues, such as muscles, face or abdomen, where the cutting of tissue can be simulated [MLM+05, MC97, NT98, Pal03]. Moreover, these systems have been used to describe a wide range of different elastic behaviors such as anisotropy [Bou03], heterogeneity [TW90], non linearity [Bou00] and also incompressibility [PBP96].

However, where FEMs are built upon elasticity theory, mass-spring models are generally far from accurate. Indeed, springs stiffness constants are generally empirically set and consequently, it is difficult to reproduce, with these models, the true behavior of a given material. Thus, if the MSS have allowed convincing animations for visualization purposes, their drawbacks refrain the generalization of their use when greater resolution is required, like for mechanical or medical simulators. An extensive review can be found in [NMK+06].

The graphics community has proposed solutions based on simulated annealing algorithms [DKT95, LPC95] to estimate spring stiffness constants to mimic correctly material properties. Usually, these solutions consist in applying random values to different springs constants and in comparing the behavior of the obtained model with some mechanical experiments in which results are either well known analytically or can be obtained numerically. Then, the stiffness constants of the springs that induce the greatest error are corrected to minimize the discrepancies. More recently, Bianchi *et al.* [BSSH04] proposed a similar approach based on genetic algorithms using reference deformations simulated with finite element methods. However, the efficiency of these approaches depends on the number of springs and is based on numerous mechanical tests leading to a quite expensive computation. Moreover, the process should be repeated after any mesh alteration and the lack of a reference solution is an obstacle to the generalization of the method to other cases.

Instead of a trial-and-error process, a formal solution that parameterizes the springs should save computer resources. In this context, two approaches were explored. The Mass-Tensor approach [CDA99, PDA03] aims at simplifying finite element method theory by a discretization of the constitutive equations on each element. Despite of its interest, this approach requires precomputations and the storage of an extensive amount of information for each mesh component (vertex, edge, face, element).

The second approach has been proposed by Van Gelder [Van98] and has been referenced in [Bou03, BO02, Deb00, MBT03, Pal03, WV97]. In this approach, Van Gelder proposes a new formulation for triangular meshes, allowing the calculation of springs stiffness constant according to elastic parameters of the object to simulate (Young's modulus E, and Poisson's ratio ν). This approach combines the advantages of an accurate mechanical parameterization with a hyper-elastic model, enabling either small or large deformations. However, numerical simulations completed by an Lagrangian analysis exhibited the incompatibility of the proposal with the physical reality [BBJ+07, Bau06]. Indeed, the Van Gelder's approach is restricted to $\nu = 0$. An extension of Van Gelder's method has been recently presented in [LSH07] for tetrahedra, hexahedra and some other common shapes, but still remains limited to $\nu = 0,3$ that prevents their use when accurate material properties are required. Finally Delingette [Del08] proposed a formal connection between springs parameters and continuum mechanics for the membranes. He succeeded to simulate realistically the behavior of a membrane for the specific case of the Poisson's ration $\nu = 0,3$ with regular MSS. The extension of this approach to 3D is not yet available.

3 OUR PARAMETERIZATION APPROACH

Our approach is based on hexahedral mesh, as currently used with the FEM. To better demonstrate the basis of our solution, we begin with the parameterization of a 2D rectangular mass-spring systems (MSS). Indeed, as in FEM, any complexes object can be obtained by the assembly of these 2D elements [Bau06]. Then, we extend our solution to 3D elements.

3.1 Case of a 2D element

At rest, the dimension of a given 2D rectangular element of our mesh is $l_0 \times h_0$. This element is composed of four edge springs with two diagonal edge springs to integrate the role of the Poisson's ratio. This configuration implies the same stiffness constant for the both diagonal springs (k_d) and an equal stiffness constant for springs laying on two parallel edges (k_{l_0} and k_{h_0}). With such boundary conditions, the elastic parameters (Young's modulus E and Poisson's ratio ν) of the bar elongated by a force $\vec{F}$, generating a stretch η and a

compression of 2δ at equilibrium, are defined by (see Fig. 1):

$$\nu = \frac{2\delta/l_0}{\eta/h_0}, \quad E = \frac{F/l_0}{\eta/h_0}. \tag{1}$$

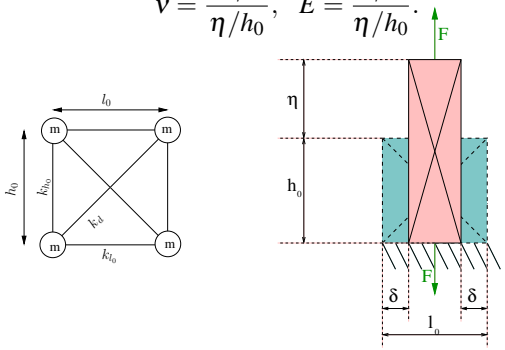

Figure 1: (Left) 2D rectangular element with three pairs of strings: k_{l_0}, k_{h_0} and k_d. (Right) Elongation test of the bar.

In addition to the Young's modulus and the Poisson's ratio, the model should simulate correctly the reaction of the object to shearing strains (correct shear modulus).

In 2D, the shearing modulus is measured by applying two opposed forces F resulting in shear stress F/l_0 on two opposite edges of the rectangular element. The material response to shearing stress is a lateral deviation with an angle θ and a displacement η (see Fig. 2).

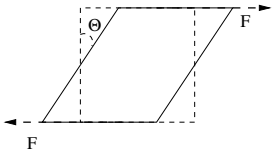

Figure 2: Experimentation to measure the 2D shear modulus: a rectangular element is subject to 2 opposed forces, generating a deviation θ and a displacement η.

Shear modulus is then defined as:

$$G = \frac{tan(\theta) \times F}{l_0} = \frac{F h_0}{l_0 \eta} \simeq \frac{\theta \times F}{l_0} \text{ when } \theta \to 0.$$

For linear elastic, isotropic and homogeneous materials, this coefficient is linked to the Young's modulus and the Poisson's ratio by $E = 2G(1+\nu)$.

Then, to determinate the spring coefficients that permit to simulate correctly these mechanical experiments, we follow these four steps [Bau06] detailed later:

1. For each experiment, we define the Lagrangian equation (sum of potential energies).
2. We apply the principle of least action to get the Newton equations.
3. We apply the definition of the measured mechanical characteristics to build a set of equations linking the spring coefficients to the mechanical characteristics.
4. Then, we solve the whole system.

First, we begin the parameterization with the shearing experiment. Indeed, only the diagonal springs are stressed in this experiment. Thus, the Lagrangian equation defining this characteristic depends only on k_d. This means that the diagonal springs are totally correlated to the shear modulus and that their stiffness constant can be calculated independently of the two others spring coefficients. The deformation of the diagonal springs is defined by:

$$\begin{aligned} \delta_d &= \sqrt{(l_0 \pm \eta)^2 + h_0^2} - \sqrt{l_0^2 + h_0^2} \\ &\sim \frac{\pm \eta l_0}{\sqrt{l_0^2 + h_0^2}} + O(n^2) \end{aligned}$$

Thus, the Lagrangian equation for the shearing is defined by:

$$L = F_\eta - k_d \frac{\eta^2 l_0^2}{l_0^2 + h_0^2}$$

Then the minimization of the energy is done for:

$$\frac{\partial L}{\partial \eta} = F - k_d \frac{2\eta l_0^2}{l_0^2 + h_0^2}$$

So we obtain:

$$\eta = \frac{F(l_0^2 + h_0^2)}{2 l_0^2 k_d}$$

Finally, using the definition of the shearing and its link with E and ν for isotropic and homogeneous materials, we obtain the following relation:

$$k_d = \frac{E\left(l_0^2 + h_0^2\right)}{4 l_0 h_0 (1+\nu)}.$$

Note that, for a square mesh element, we obtain:

$$k_d = \frac{E}{2(1+\nu)} = G.$$

Then, we continue the parameterization to find k_{l_0} and k_{h_0} by doing two elongation experimentations in lateral and longitudinal direction. We obtain four equations with two equations from each elongation experiment [Bau06]. This over-constrained system admits one solution for $\nu = 0.3$, as stated by Lloyd *et al.* [LSH07] and Delingette [Del08]. This result is not satisfactory because we wish to simulate the behavior of any real material. Consequently, we have to add two degrees of freedom to solve this problem.

We note that the Poisson's ratio defines the thinning at a given elongation, *i. e.* it determines the forces orthogonal to the elongation direction. Thus, we introduced for each direction a new variable that represents this orthogonal force. The force orthogonal to h_0 (*resp.* l_0) is noted $F_{\perp h_0}$(*resp.* $F_{\perp l_0}$) (see Fig. 3). Thus, the addition of these 2 new variables leads to a system of 4

equations with 4 unknowns. Note that this kind of correction is equivalent to the reciprocity principle used in finite elements methods [Fey64].

For a constraint F_{h_0} according to h_0, we obtain the following Lagrangian equation:

$$L = F_{h_0}\eta - 4F_{\perp h_0}(2\delta) - 4k_{l_0}\delta^2 - k_{h_0}\eta^2 - k_d\left(\frac{h_0\eta - 2l_0\delta}{\sqrt{h_0^2+l_0^2}}\right)^2.$$

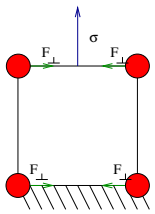

Figure 3: Correction forces.

By following the same line as for the shearing Lagrangian, we find the expressions of η and δ. Then, using the definitions of the Young modulus and the Poisson's ratio, we obtain k_{l_0} and k_{h_0}, but according to this new potential. By setting the symmetry of k_{l_0} with k_{h_0}, we can restrain $F_\perp$ and obtain the relations for k_{l_0}, k_{h_0} and $F_{\perp h_0}$. Note that, the experimentation according to l_0 permits to obtain the same stiffness constants and formulation for the corrective force. Finally, the solution of the new system is (with $(i,j) \in \{l_0, h_0\}^2$ with $i \neq j$):

$$k_i = \frac{E\left(j^2(3\nu+2) - i^2\right)}{4\, l_0\, h_0\,(1+\nu)}, \quad F_{\perp i} = \frac{i\, F_i\,(1-3\nu)}{8j}.$$

As said before, the symmetry involves that the 6 springs of each element are only defined by three spring coefficients and the elongation/compression correction forces.

3.2 Generalisation to 3D elements

Our 3D model is the generalization of our 2D approach, by the use of parallelepiped elements. Let's consider this element with rest dimensions $x_0 \times y_0 \times z_0$. As in 2D, to ensure homogeneous behavior, springs laying on parallel edges need to have the same stiffness constant. Thus, we have to determine only 3 stiffness coefficients for these edges: k_{x_0}, k_{y_0} and k_{z_0}. In addition, some diagonal springs are necessary to reproduce the thinning induced by the elongation. Fig.4 displays three possible configurations for these diagonal links:

- diagonal springs located on all the faces (M1),
- only the inner diagonals (M2),
- the combination of both inner and face diagonals (M3).

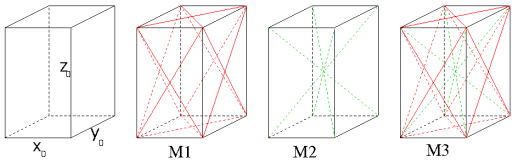

Figure 4: Three possible configurations for integrating the diagonal links in the 3D element composition.

Prior to the above configuration choice, let's present our springs parameterization approach. As in 2D, we propose a methodology within the Lagrangian framework, and according to the following procedure. For each experiment that defines an elastic characteristic:

1. We build the Lagrangian as the sum of the potential of springs due to elongation as well as the potential of external forces, since kinetic term is null.
2. We establish a Taylor's expansion of the Lagrangian to the second order in deformations and apply the principle of least action. It reads linear equations.
3. We obtain a set of equations, since the mechanical characteristics are input parameters. We solve this system to get stiffness coefficients.

To solve the system, the number of unknowns has to be equal to the number of equations (constraints). Three equations result from each elongation experiment (one for the Young's modulus and one for the Poisson's ratio along each direction orthogonal to the elongation). Thus, we obtain 9 equations for all the elongation directions. Moreover, 6 more equations have to be added to take into account the shear modulus (6 experiments).

Three degrees of freedom stem from the parallel edge (k_{x_0}, k_{y_0}, k_{z_0}), but the total number of freedom degrees depends on the diagonal spring configuration. Note that, for small shearing ($\theta \approx 0$), only diagonal springs are stressed. Thus, the Lagrangian equation defining this characteristic depends only on the stiffness constants k_{d_i} of the different diagonals. This means that the diagonal springs constant can be determined independently of the other stiffness coefficients.

	M1	**M2**	**M3**
Nb of unknown for shearing	3	1	4
Nb of unknown for elongation	3+(3)	3+(1)	3+(4)
Total nb of unknown stiffness cst.	6	4	7
Nb of equations for elongation	9	9	9
Nb of equations for shearing	6	3	6
Total number of equations	15	12	15

Table 1: Number of equations and unknowns according to the chosen geometry.

We summarize the number of degrees of freedom and the number of equations in Table 1 according to the possible configurations of the system. We observe

that all the geometrical configurations bring to an over-constraint system. Nevertheless, the configuration (M2) is less constrained than the others. Thus, we chose this configuration which corresponds to the model with only the inner diagonals in which the 4 diagonal springs have the same stiffness constant noted k_d.

Like in 2D, we begin the parameterization with the shearing experiment. As mentioned above, the inner diagonals fully define the shearing modulus. The problem is that there is only 1 diagonal spring variable for 3 shearing equations (see Table 1). Each equation, corresponding to one particular direction i ($i \in \{x_0, y_0, z_0\}$), leads to a different solution (using the same reasoning as in 2D):

$$k_{d_i} = \frac{E\, i \sum_{j\in\{x_0,y_0,z_0\}} j^2}{8(1+\nu)\Pi_{\{l\in\{x_0,y_0,z_0\},l\neq i\}} l}.$$

However an unique solution can be obtained for a cubic element (*i. e.* with $x_0 = y_0 = z_0$). In this case k_d is well defined proportionally to G, with:

$$k_d = \frac{3Ex_0}{8(1+\nu)}. \tag{2}$$

Thus, we constrain the mesh element to a cube and we continue our parameterization with the elongation experimentations to obtain the stiffness constants of the others edge springs. The non-diagonal edges are identical and their spring stiffness constant is noted k_x. This stiffness coefficient has to satisfy two relations (E and ν). One solution can be found for the Poisson's ratio $\nu = 0.25$ but this is not a versatile solution, thus unsatisfying (a complete demonstration can be found in Appendix A).

Since the number of equations is greater than the number of degrees of freedom, we introduce as in 2D, correction forces. Thus, two new forces induced by the elongation are added. For the sake of symmetry, the amplitude of the forces is identical in both directions. This amplitude $F_\perp$ is the new degree of freedom (see Fig. 3).

This new additional variable leads to a system of 2 equations with 2 unknowns. After resolution, we obtain the following relations for $i \in \{x_0, y_0, z_0\}$ (using the same reasoning as in 2D):

$$k_x = \frac{Ex(4\nu+1)}{8(1+\nu)},\ F_{\perp i} = -\frac{F_i(4\nu-1)}{16}.$$

Since all the stiffness coefficients and the added compressive forces are now determined for a mesh element, we can tackle the simulation of any object composed of mesh elements. Then, the simulation of an object results from the simulation of the deformation of each single element that constitutes the object. For this, we need to:

1. Compute all the forces applied to an element. These forces can be (i) internal, including forces due to springs and correction forces, or (ii) external, like gravity or reaction forces due to neighborhood.

2. Calculate accelerations and velocities according to a numerical integration scheme such as explicit or implicit Euler scheme, Verlet method, ...

3. Displace each mesh node consequently.

Note that, to compute the correction forces applied to a mesh element face, we need to compute the elongation force. This elongation force is the component of the sum of all applied forces to a face, in the direction of face normal vector.

The next section will describe numerical experimentations.

4 EVALUATION OF THE 3D MODEL

We propose now to qualify the mechanical properties of our system. For this, we have carried out several tests. Note that, we do not provide some performance results, because the main advantage of our method is to propose a solution that do not add any cost in a classical animation.

Deflection experiment

The deflection experience (construction or structural element bends under a load) is recommended to validate mechanical models. It constitutes a relevant test to evaluate (a) the mass repartition, and (b) the behavior in case of large deformations (inducing large rotations, especially close to the fixation area).

This test consists in observing the deformation of a beam anchored at one end to a support. At equilibrium, under gravity loads, the top of the beam is under tension while the bottom is under compression, leaving the middle line of the beam relatively stress-free. The length of the zero stress line remains unchanged (see Fig. 5).

In case of a null Poisson's ratio, the load induced deviation of the neutral axis is given by:

$$y(x) = \frac{\rho g}{24\, EI}\left(6\, L^2x^2 - 4\, L\, x^3 + x^4\right) \tag{3}$$

for a parallelepiped beam of inertia moment $I = TH^3/12$, and with linear density $\rho = M/L$.

We notice that results are dependent of the sampling resolution, as for any other numerical method, however the fiber axis profile keeps close to the profile given by equation (3). Figure 5 displays some results for a cantilever beam of dimensions $400\times100\times100$ mm, with Young's modulus equals to 1000 Pa, Poisson's ratio to 0.3 and a mass of 0.0125 Kg.m^{-3}. By looking at the displacement errors at each mesh node, we observe that the error is decreasing when the sampling is improved:

the maximum error in the sampling $4 \times 1 \times 1$ is about 45% while it is about 5% compared to a FEM reference result, for a resolution of $16 \times 4 \times 4$, proving again the convergent behavior of our technique.

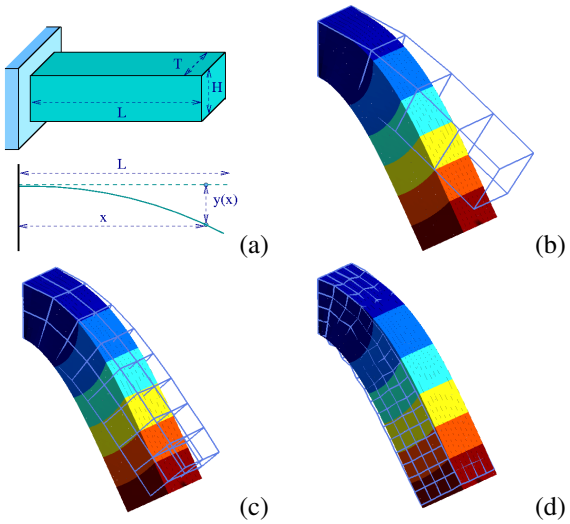

(b) 4×1×1: M=16.31%, SD=2.83%, MAX=38%.
(c) 8×2×2: M=7.08%, SD=0.58%, MAX=16.7%.
(d) 16×4×4: M=0.68%, SD=0.03%, MAX=4.05%.

Figure 5: Deflection experiment: (a) Cantilever neutral axis deviation, (b-d) the reference FEM solution (in color gradation) with superimposition of various simulations performed for different sampling resolutions (wire mesh).

Shearing experiment: Illustration on a non-symmetric composition

For the shearing experiment, we have chosen a L-like object fixed at its base. We apply a constant force to the edges orthogonal to the base. Figure 6 shows our results superimposed to the FEM solution, with a map of error in displacement. The object dimensions are 4000×4000×4000mm. The mechanical characteristics are: Young's modulus of 1kPa, Poisson's ratio of 0.3 and an applied force of 0.3GN. In this experiment, we have neglected the mass. Again we clearly observe that our model behaves as expected: better mesh resolution leads to better results. Moreover, the dissymmetry of the geometry does not influence the accuracy of the results.

3D deformable object simulation

An example of application is depicted on Fig. 7. By dragging points, we applied some external forces on an initial hexahedral meshing of a puma, leading to produce the head lateral movement. Note that the initial choice of a parallelepiped shape is absolutely not a constraint in most applications. This choice has been motivated by the fact that it is considered by the numerical community as stable and more precise for the same number of elements than a tetrahedral mesh element. This is to be counterbalanced by the fact that it requires generally more elements to fit a non simple geometry. Anyway, for better visualization or collision detection purposes, it is easy to fit a triangular skin on our hexahedral model, as shown on Fig. 7.

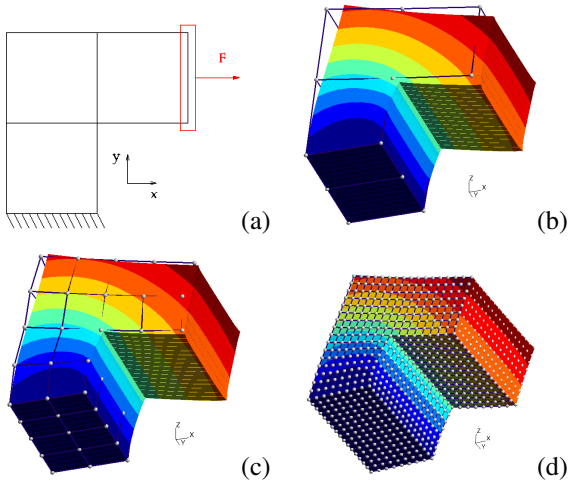

(b) 2×2×2: M=6.99%, SD=0.94%, MAX=18%.
(c) 4×4×4: M=3.37%, SD=0.20%, MAX=7%.
(d) 8×8×8: M=0.66%, SD=0.01%, MAX=1.6%.

Figure 6: Experiment on a non-symmetric object: (a) load scheme, (b-d) the reference FEM solution (in color gradation) with superimposition of various simulations performed for different mesh resolutions.

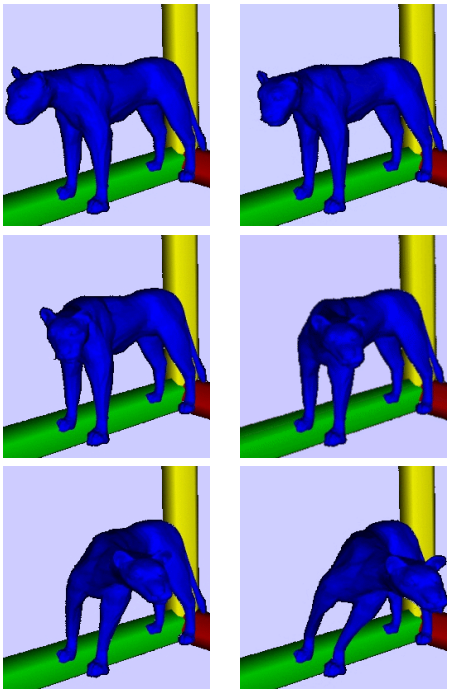

Figure 7: A complete 3D application: simulation of the head lateral movement at different steps.

5 CONCLUSION AND FUTURE WORK

We proposed a mass-spring model that ensures fast and physically accurate simulation of linear elastic, isotropic and homogeneous material. It consists in meshing any object by a set of cubic mass-spring elements. By construction, our model is well characterized by the Young's modulus and Poisson's ratio. The spring coefficients have just to be initialized according to simple analytic expressions. The precision of our model have been given, by comparing our results with those obtained by a finite element method, chosen as reference.

In the future, we are looking to apply the same techniques to other geometrical elements, for example tetrahedron or any polyhedron. This would increase the geometrical reconstruction possibilities and would offer more tools for simulating complex shapes, although in the actual state, the hexahedral shape is not a constraint in many applications ranging from mechanics to medicine. If desired, a triangulation of the surface can be performed with ease and at reduced computational cost.

Mesh optimization or local mesh adaptation would probably improve the efficiency of the model. For example, we can modify the resolution in the vicinity of highly deformed zones, reducing large rotations of elements undergoing heavy load.

We exhibited that our model can support reasonably large deformations. The accuracy increases with the mesh resolution. This is a major improvement relatively to early techniques, as it is generally dependent to the mesh resolution and topology. However, it may be interesting to investigate a procedure to update the spring coefficients and corrective forces when the deformations become too large. In this case, the elastic behaviour will be lost (the initial shape will not be recovered), but this may allow to handle strong topology alteration, even melting.

APPENDIX A

Demonstration: nonexistence of a 3D general solution

Being a cubic element with edge of length x_0. Consequently, face diagonals are of length $d_{face} = \sqrt{2}\,x_0$, and cube diagonals $d_{cube} = \sqrt{3}\,x_0$. Spring stiffness are equal along the edges ($K_x = K_y = K_z$), as well for faces: ($K_{xy} = K_{xz} = K_{yz}$, denoted K_{xx}).

By symmetry in the cube, all 6 shearings are equivalent and can be resumed into a single equation. A shearing stress due to a sliding η leads to the deformation of the 4 cube diagonals as well as the 4 diagonals of the 2 lateral faces, respectively $\Delta_{d_{cube}}$ and $\Delta_{d_{face}}$:

$$\begin{aligned} \Delta_{d_{cube}} &= \sqrt{(x+\eta)^2+2x^2} - \sqrt{3}\,x \sim \tfrac{\sqrt{3}}{3}\eta \\ \Delta_{d_{face}} &= \sqrt{(x+\eta)^2+x^2} - \sqrt{2}\,x \sim \tfrac{\sqrt{2}}{2}\eta \end{aligned}$$

The static Lagrangian linked to shearing is reckoned in the following way:

$$L = F_{cis}\eta - \frac{4K_d}{2}\frac{\eta^2}{3} - \frac{4K_{xx}}{2}\frac{\eta^2}{2}$$

After resolution, they find the equation of shearing in K_{xx} and K_d:

$$\frac{4K_d + 6K_{xx}}{3x} = \frac{E}{2(1+\nu)} \tag{4}$$

We can consequently incorporate the compressibility law. For this, we apply an uniform pressure to the cube, which generates an uniform distortion η. This deformation leads as well to the (identical) deformation of all the diagonals:

$$\begin{aligned} \Delta_{d_{cube}} &= \sqrt{3(x+\eta)^2} - \sqrt{3}\,x \sim \sqrt{3}\,\eta \\ \Delta_{d_{face}} &= \sqrt{2(x+\eta)^2} - \sqrt{2}\,x \sim \sqrt{2}\,\eta \end{aligned}$$

Pressures being applied at each face are equal and this implicates the same surface force F_{face}. The Lagrangian is as follows:

$$L = 3F_{face}\eta - \frac{12K_x}{2}\eta^2 - \frac{12K_{xx}}{2}2\eta^2 - \frac{4K_d}{2}3\eta^2$$

After resolution, compressibility equation is:

$$\begin{aligned} K &= -\frac{\Delta P}{\Delta V/V_0}\frac{F_{face}/(x+\eta)^2}{\left((x+\eta)^3 - x^3\right)/x^3} \sim \frac{F_{face}}{3x\eta} \\ &= \frac{E}{3(1-2\nu)} \end{aligned}$$

Hence,

$$\frac{4K_x + 8K_{xx} + 4K_d}{3x} = \frac{E}{3(1-2\nu)} \tag{5}$$

We can now deal with equations governing a tensile stress η; by symmetry other directions are compressed of the same value, δ. So, two faces ($face_2$) are shrieked by keeping their square shape, while the other 4 are stretched ($face_1$). Diagonals are deformed in the following way:

$$\begin{aligned} \Delta_{d_{cube}} &= \sqrt{(x+\eta)^2+2(x-2\delta)^2} - \sqrt{3}\,x \sim \tfrac{\sqrt{3}}{3}\eta - \tfrac{4\sqrt{3}}{3}\delta \\ \Delta_{d_{face_1}} &= \sqrt{(x+\eta)^2+(x-2\delta)^2} - \sqrt{2}\,x \sim \tfrac{\sqrt{2}}{2}\eta - \sqrt{2}\,\delta \\ \Delta_{d_{face_2}} &= \sqrt{2(x-2\delta)^2} - \sqrt{2}\,x \sim -2\sqrt{2}\,\delta \end{aligned}$$

 ISBN 978-80-86943-93-0

The Lagrangian associated to the tensile experiment:

$$\begin{aligned} L &= F\eta - 2K_x\eta^2 - 16K_x\delta^2 - 16K_{xx}\delta^2 \\ &\quad -4K_{xx}\left(\frac{\sqrt{2}}{2}\eta - \sqrt{2}\,\delta\right)^2 - 2K_d\left(\frac{\sqrt{3}}{3}\eta - \frac{4\sqrt{3}}{3}\delta\right)^2 \end{aligned}$$

After resolution, Young modulus and Poisson ratio definitions lead to:

$$\begin{aligned} E &= \frac{12K_dK_{xx} + 24K_{xx}^2 + 24K_x^2 + 60K_xK_{xx} + 24K_xK_d}{x\,(6K_x + 9K_{xx} + 4K_d)} \\ \nu &= \frac{2K_d + 3K_{xx}}{6K_x + 9K_{xx} + 4K_d} \end{aligned} \quad (6)$$

These equations (eq. (4), (5) and (6)) cannot be solved (except for $\nu = 0.25$), what establish a strong result, since it implicates that it is unfortunately not possible to reproduce an elastic homogeneous behavior only with this simplistic model. As in 2D corrective forces should be introduced.

Aknowledgements

We thank the ETOILE (Espace de Traitement Oncologique par Ions Légers, http://www.centre-etoile.org/) project for its support.

REFERENCES

[Bau06] Vincent Baudet. *Modélisation et simulation paramétrable d'objets déformables*. PhD thesis, Université Lyon 1, 2006.

[BBJ+07] Vincent Baudet, Michaël Beuve, Fabrice Jaillet, Behzad Shariat, and Florence Zara. A new mass-spring system integrating elasticity parameters in 2d. Technical Report RR-LIRIS-2007-003, February 2007.

[BO02] Cynthia Bruyns and Mark Ottensmeyer. Measurements of soft-tissue mechanical properties to support development of a physically based virtual anima model. In *MICCAI 2002*, pages 282–289, 2002.

[Bou00] François Boux de Casson. *Simulation dynamique de corps biologiques et changements de topologie interactifs*. PhD thesis, Université de Savoie, 2000.

[Bou03] David Bourguignon. *Interactive Animation and Modeling by Drawing - Pedagogical Applications in Medicine*. PhD thesis, Institut National Polytechnique de Grenoble, 2003.

[BSSH04] Gérald Bianchi, Barbara Solenthaler, Gàbor Székely, and Matthias Harders. Simultaneous topology and stiffness identification for mass-spring models based on FEM reference deformations. In Springer-Verlag, editor, *MICCAI 2004*, pages 293–301, Berlin, 2004.

[CDA99] Stéphane Cotin, Hervé Delingette, and Nicholas Ayache. Efficient linear elastic models of soft tissues for real-time surgery simulation. *Proceedings of the Medecine Meets Virtual Reality (MMVR 7)*, 62:100–101, 1999.

[Deb00] Gilles Debunne. *Animation multirésolution d'objets déformables en temps réel, Application à la simulation chirurgicale*. PhD thesis, Institut National Polytechnique de Grenoble, 2000.

[Del08] Herve Delingette. Triangular springs for modeling nonlinear membranes. *IEEE Transactions on Visualization and Computer Graphics*, 14(2):329–341, 2008.

[DKT95] O. Deussen, L. Kobbelt, and P. Tucke. Using simulated annealing to obtain good nodal approximations of deformable objects. In Springer-Verlag, editor, *Proceedings of the Sixth Eurographics Workshop on Animation and Simulation*, pages 30–43, Berlin, 1995.

[Fey64] R. Feynman. *The Feynman Lectures on Physics*, volume 2. Addison Wesley, 1964. chapter 38.

[KEH04] Michael Keckeisen, Olaf Etzmuß, and Michael Hauth. Physical models and numerical solvers for cloth animations. In *Simulation of Clothes for Real-time Applications*, volume Tutorial 1, pages 17–34. INRIA and the Eurographics Association, 2004.

[LJF+91] A. Luciani, S. Jimenez, J. L. Florens, C. Cadoz, and O. Raoult. Computational physics: A modeler-simulator for animated physical objects. In *Proceedings of Eurographics 91*, pages 425,436, Amsterdam, 1991. Eurographics.

[LPC95] Jean Louchet, Xavier Provot, and David Crochemore. Evolutionary identification of cloth animation models. In Springer-Verlag, editor, *Proceedings of the Sixth Eurographics Workshop on Animation and Simulation*, pages 44–54, Berlin, 1995.

[LSH07] B.A. Lloyd, G. Székely, and M. Harders. Identification of spring parameters for deformable object simulation. *IEEE Trans. on Visualization and Computer Graphics*, 13(5):1081–1094, Sept-Oct 2007.

[MBT03] Anderson Maciel, Ronan Boulic, and Daniel Thalmann. *Deformable Tissue Parameterized by Properties of Real Biological Tissue*, volume 2673 of *Lecture Notes in CS: Surgery Simulation and Soft Tissue Modeling*, pages 74–87. Springer, 2003.

[MC97] Philippe Meseure and Christophe Chaillou. Deformable body simulation with adaptative subdivision and cuttings. In *5th Int. Conf. in Central Europe on Comp. Graphics and Visualisation WSCG'97*, pages 361–370, 1997.

[MLM+05] U. Meier, O López, C. Monserrat, M. C. Juan, and M. Alcañiz. Real-time deformable models for surgery simulation : a survey. *Computer Methods and Programs in Biomedicine*, 77(3):183–197, 2005.

[NMK+06] A. Nealen, M. Müller, R. Keiser, E. Boxerman, and M. Carlson. Physically based deformable models in computer graphics. *Computer Graphics Forum*, 25(4):809–836(28), December 2006.

[NT98] L. Porcher Nedel and D. Thalmann. Real-time muscles deformations using mass-spring systems. *Computer Graphics International*, pages 156–165, 1998.

[Pal03] Céline Paloc. *Adaptative Deformable Model (allowing Topological Modifications) for Surgical Simulation*. PhD thesis, University of London, 2003.

[PBP96] Emmanuel Promayon, Pierre Baconnier, and Claude Puech. Physically based deformation constrained in displacements and volume. In *Proceedings of Eurographics'96*, Oxford, 1996. BlackWell Publishers.

[PDA03] Guillaume Picinbono, Hervé Delingette, and Nicholas Ayache. Non-linear anisotropic elasticity for real-time surgery simulation. *Graphical Model*, 2003.

[Pro95] Xavier Provot. Deformation constraints in a mass-spring model to describe rigid cloth behavior. In *Proceedings of Graphics Interface 95*, pages 147,154, Toronto, 1995. Canadian Human-Computer Communications Society.

[TW90] D. Terzopoulos and K. Waters. Physically-based facial modelling, analysis, and animation. *The Journal of Visualization and Computer Animation*, 1:73–80, 1990.

[Van98] Allen Van Gelder. Approximate simulation of elastic membranes by triangulated spring meshes. *Journal of Graphics Tools*, 3(2):21–42, 1998.

[WV97] Jane Wilhelms and Allen Van Gelder. Anatomically based modelling. In *Computer Graphics (SIGGRAPH'97 Proceedings)*, pages 173–180, 1997.